

# Active Rectifier Inner Current Loop without Reference Frame Transformations in Feedback

Eric Seymour  
Advanced Energy Industries  
1625 Sharp Point Dr  
Fort Collins, CO 80525, USA  
[eric.seymour@aei.com](mailto:eric.seymour@aei.com)

Annabelle Pratt  
Advanced Energy Industries  
1625 Sharp Point Dr  
Fort Collins, CO 80525, USA  
[apratt@ieee.org](mailto:apratt@ieee.org)

**Abstract-** The effective control of an active rectifier requires a control system capable of a number of high-speed real-time operations including multiple reference frame transformations. This paper presents a cost-effective, computationally efficient method of control for active rectifiers. An analytical comparison is provided of the technique with respect to an established active rectifier control method followed by a comparison of performance characteristics.

## I. INTRODUCTION

The control of active rectifiers such as that shown in Figure 1, is typically implemented with an inner current loop capable of fast line current control and slower outer loops which control the DC bus voltage  $v_{DC}$  and input reactive power flow. In order to decouple the two outer loops, the control is typically implemented in the synchronous  $dq$  reference frame, which requires data-acquisition and processing systems to perform reference frame conversion at speed sufficient to support inner loop control bandwidth. This paper proposes an inner current loop control scheme which does not require reference frame conversion in the feedback, allowing a lower cost implementation since the hardware does not need to be as fast. The proposed control scheme approximates the behavior of *full state feedback control*.

Figure 2 shows the state space model in the synchronous  $dq$  frame for the proposed inner current loop. Quantities in the  $abc$  frame  $\mathbf{x}_{abc}$  are converted to quantities in the synchronous  $dq$  frame  $\mathbf{x}$  as shown in (1).  $T_s$  converts quantities from the  $abc$  to the stationary  $dq$ , or  $\alpha\beta$ , frame, and  $T_e(\theta)$  converts quantities from the  $\alpha\beta$  frame to the synchronous  $dq$  frame, where  $\theta$  is a phase locked loop (PLL) derived conversion angle.

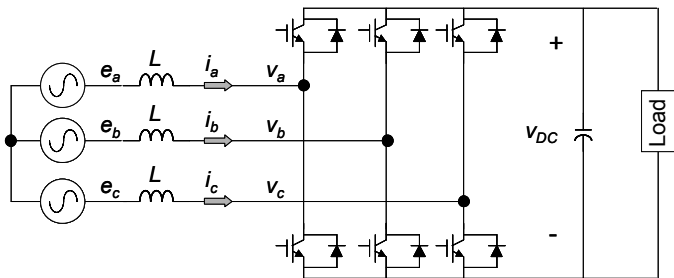


Figure 1 Active rectifier circuit

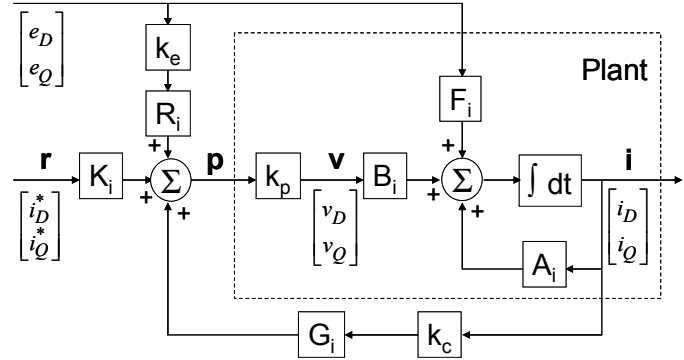


Figure 2 State space model of proposed inner current loop

Inverse transformations are applied to convert from the synchronous  $dq$  back to the  $abc$  frame.

$$\mathbf{x} = \begin{bmatrix} x_D \\ x_Q \end{bmatrix} = T_e(\theta) T_s \begin{bmatrix} x_a \\ x_b \\ x_c \end{bmatrix} = T_e(\theta) T_s \mathbf{x}_{abc} \quad (1)$$

where

$$T_s = \frac{2}{3} \begin{bmatrix} 1 & -\frac{1}{2} & -\frac{1}{2} \\ 0 & \frac{\sqrt{3}}{2} & \frac{\sqrt{3}}{2} \end{bmatrix}$$

and

$$T_e(\theta) = \begin{bmatrix} \cos \theta & -\sin \theta \\ -\sin \theta & -\cos \theta \end{bmatrix}$$

The outer control loops generate references for the line currents  $\mathbf{r} = [i_D^* \ i_Q^*]^T$ . With appropriate design of gain matrices  $G_i$  and  $K_i$ , the inner current loop ensures that the line currents  $\mathbf{i} = [i_D \ i_Q]^T$  track the references by issuing the appropriate control signals  $\mathbf{p}$ , as shown in Figure 2. The line voltages  $\mathbf{e}$  act as disturbances to the system, and  $R_i$  is designed to provide disturbance rejection. The constants  $k_e$  and  $k_c$  are voltage and current measurement gains respectively. It is assumed that the inverter voltages  $\mathbf{v}$  follow the control signals  $\mathbf{p}$  perfectly, so the active rectifier is modeled as a simple gain  $k_p$ , i.e.

$$\mathbf{v} = k_p \mathbf{p}$$

The state space equations for the plant in the synchronous  $dq$  frame are

$$\begin{aligned} \frac{d}{dt} \begin{bmatrix} i_D \\ i_Q \end{bmatrix} &= \begin{bmatrix} 0 & -\omega \\ \omega & 0 \end{bmatrix} \begin{bmatrix} i_D \\ i_Q \end{bmatrix} - \begin{bmatrix} \frac{1}{L} & 0 \\ 0 & \frac{1}{L} \end{bmatrix} \begin{bmatrix} v_D \\ v_Q \end{bmatrix} \\ &+ \begin{bmatrix} \frac{1}{L} & 0 \\ 0 & \frac{1}{L} \end{bmatrix} \begin{bmatrix} e_D \\ e_Q \end{bmatrix} \\ \frac{d\mathbf{i}}{dt} &= A_i \mathbf{i} + B_i \mathbf{v} + F_i \mathbf{e} \end{aligned}$$

where  $\omega = d\theta/dt$ . It can be seen from the off-diagonal terms in  $A_i$  that there is cross coupling between the  $d$  and  $q$  axes. An important goal of feedback in the inner current loop is to cancel this cross coupling. The plant is type 0, i.e. it has no integrator in the plant, so external integration would need to be added to ensure zero steady state error if the system model is not correct [1,2]. Since the outer loops will have integration terms driving the system outputs to their setpoints (the output voltage and input reactive power), it is not necessary to achieve zero steady state error in the inner loop, and full state feedback can be used [2].

## II. FULL STATE FEEDBACK CONTROL IMPLEMENTATION

The desired closed loop system is decoupled with both the  $d$  and  $q$  axis current loops having a single pole at  $s = -a_c$ . Similar response is required for the  $d$  and  $q$  axis currents, so they are assigned the same pole location. The desired system equations are

$$\begin{aligned} \frac{d}{dt} \begin{bmatrix} i_D \\ i_Q \end{bmatrix} &= \begin{bmatrix} -a_c & 0 \\ 0 & -a_c \end{bmatrix} \begin{bmatrix} i_D \\ i_Q \end{bmatrix} + \begin{bmatrix} a_c & 0 \\ 0 & a_c \end{bmatrix} \begin{bmatrix} i_D^* \\ i_Q^* \end{bmatrix} \\ &+ \begin{bmatrix} 0 & 0 \\ 0 & 0 \end{bmatrix} \begin{bmatrix} e_D \\ e_Q \end{bmatrix} \\ \frac{d\mathbf{i}}{dt} &= A_c \mathbf{i} + B_c \mathbf{r} + F_c \mathbf{e} \end{aligned} \quad (2)$$

In placing the closed loop pole, the following requirements need to be met:

1. The inner loop bandwidth should be faster than the outer loop bandwidth. The outer loop response time is desired to be a quarter cycle, i.e. 4 msec, and assuming a first order transfer function for the outer loop, the outer loop bandwidth  $f_{co}$  is related to the settling time  $t_s$  (2% criterion) as follows [4, p.254]

$$t_s = \frac{4}{2\pi f_{co}} = 4 \text{ msec} \Rightarrow f_{co} = 160 \text{ Hz}$$

For an inner loop bandwidth  $f_{ci}$  ten times higher than the outer loop bandwidth,

$$f_{ci} = \frac{a_c}{2\pi} > 10 \times f_{co} = 1.6 \text{ kHz}$$

2. Attenuation is needed at the switching frequency, which is 18kHz, so the inner loop bandwidth should be significantly lower than the switching frequency. For a bandwidth four times lower,  $f_{ci} < 18\text{kHz} / 4 = 4.5\text{kHz}$ .

3. The bandwidth should be below the Nyquist frequency, which is half the sampling rate to prevent aliasing. The phase delay due to sampling degrades the phase margin, so the bandwidth is in practice limited to below an eighth of the sampling frequency. In order to achieve a bandwidth  $f_{ci}$  of 4.5kHz, a sampling rate of at least  $8 \times 4.5\text{kHz} = 36\text{kHz}$  would therefore be required.

The form of the control signals required to achieve the system in (2) using full state feedback are

$$\mathbf{p} = G_i k_c \mathbf{i} + K_i \mathbf{r} + R_i k_e \mathbf{e}$$

This will result in the following closed loop system

$$\begin{aligned} \frac{d\mathbf{i}}{dt} &= A_i \mathbf{i} + B_i \mathbf{v} + F_i \mathbf{e} = A_i \mathbf{i} + B_i k_p \mathbf{p} + F_i \mathbf{e} \\ &= A_i \mathbf{i} + B_i k_p (G_i k_c \mathbf{i} + K_i \mathbf{r} + R_i k_e \mathbf{e}) + F_i \mathbf{e} \\ &= (A_i + B_i k_p G_i k_c) \mathbf{i} + B_i k_p K_i \mathbf{r} + (B_i k_p R_i k_e + F_i) \mathbf{e} \\ &= A_c \mathbf{i} + B_c \mathbf{v} + F_c \mathbf{e} \end{aligned}$$

By setting this system equal to the desired system in (2), the required matrices are determined as follows

$$\begin{aligned} \mathbf{p} &= G_i k_c \mathbf{i} + K_i \mathbf{r} + R_i k_e \mathbf{e} \\ &= \frac{L}{k_p k_c} \begin{bmatrix} a_c & -\omega \\ \omega & a_c \end{bmatrix} k_c \mathbf{i} + \frac{-L}{k_p} \begin{bmatrix} a_c & 0 \\ 0 & a_c \end{bmatrix} \mathbf{r} \\ &+ k_r \mathbf{I} k_e \mathbf{e} \end{aligned} \quad (3)$$

where  $k_r = 1/k_p k_e$  and  $\mathbf{I}$  is the identity matrix.  $G_i$  contains off-diagonal terms which provide cancellation of cross coupling between the  $d$  and  $q$  axes. Note that if the system model is not correct, which may be the case due to component variation, there will be some cross coupling, non-zero steady state error, and line voltage disturbance rejection will not be complete.

The control signals  $\mathbf{p}$  for full state feedback are generated in the synchronous  $dq$  frame, but need to be transformed to the  $abc$  frame in order to generate the PWM signals for the active rectifier with an analog PWM implementation, i.e.

$$\begin{aligned} \mathbf{p}_{abc} &= T_s^{-1} T_e^{-1}(\theta) \mathbf{p} \\ &= T_s^{-1} T_e^{-1}(\theta) \{G_i k_c \mathbf{i} + K_i \mathbf{r} + R_i k_e \mathbf{e}\} \end{aligned}$$

The currents  $\mathbf{i}$  and line voltages  $\mathbf{e}$  are required in the  $dq$  frame to synthesize the control signal  $\mathbf{p}$ , so they need to be transformed from the  $abc$  frame to the  $dq$  frame. Since  $\mathbf{r}$  is generated in the  $dq$  frame by the outer loop, there is no need to transform it. However, since  $R_i$  has no off-diagonal terms, it is shown below that the line voltages  $\mathbf{e}$  do not need to go through any transformations, simplifying the implementation, as shown in Figure 3 for a full state feedback implementation.

$$\begin{aligned}\mathbf{p}_{abc} &= T_s^{-1} T_e^{-1}(\theta) \{G_i k_c T_e(\theta) T_s \mathbf{i}_{abc} + K_i \mathbf{r}\} \\ &\quad + T_s^{-1} T_e^{-1}(\theta) k_r \mathbf{I} k_e T_e(\theta) T_s \mathbf{e}_{abc} \\ &= T_s^{-1} T_e^{-1}(\theta) \{G_i T_e(\theta) T_s k_c \mathbf{i}_{abc} + K_i \mathbf{r}\} \\ &\quad + k_r k_e \mathbf{e}_{abc}\end{aligned}$$

### III. APPROXIMATION OF FULL STATE FEEDBACK

Consider more closely the method by which decoupling is achieved in full state feedback. Assuming that complete disturbance rejection of  $\mathbf{e}$  is achieved, i.e.  $F_c = 0$ , the system model simplifies to

$$\begin{aligned}\frac{d\mathbf{i}}{dt} &= A_c \mathbf{i} + B_c \mathbf{r} = (A_i + B_i k_p G_i k_c) \mathbf{i} + B_c \mathbf{r} \\ \frac{d}{dt} \begin{bmatrix} i_D \\ i_Q \end{bmatrix} &= \left( \begin{bmatrix} 0 & -\omega \\ \omega & 0 \end{bmatrix} + \begin{bmatrix} -a_C & \omega \\ -\omega & -a_C \end{bmatrix} \right) \begin{bmatrix} i_D \\ i_Q \end{bmatrix} \\ &\quad + \begin{bmatrix} a_C & 0 \\ 0 & a_C \end{bmatrix} \begin{bmatrix} i_D^* \\ i_Q^* \end{bmatrix}\end{aligned}\quad (4)$$

The terms  $-\omega i_Q$  and  $+\omega i_D$  are the cross coupling terms introduced by the system in  $di_D/dt$  and  $di_Q/dt$  respectively. The terms  $+\omega i_Q$  and  $-\omega i_D$  are introduced in  $di_D/dt$  and  $di_Q/dt$  respectively by the feedback in order to de-couple the system.

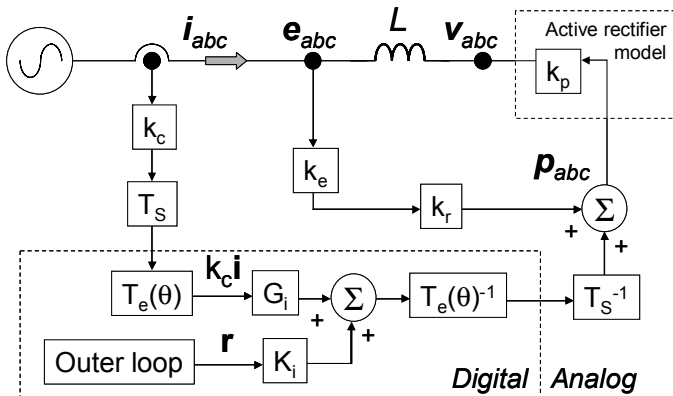


Figure 3 Implementation of full state feedback

This paper proposes an alternative method in which the terms  $+\omega i_Q^*$  and  $-\omega i_D^*$  are used instead to achieve approximate decoupling, and a system as follows is achieved.

$$\begin{aligned}\frac{d}{dt} \begin{bmatrix} i_D \\ i_Q \end{bmatrix} &= \left\{ \begin{bmatrix} 0 & -\omega \\ \omega & 0 \end{bmatrix} + \begin{bmatrix} -a_C & 0 \\ 0 & -a_C \end{bmatrix} \right\} \begin{bmatrix} i_D \\ i_Q \end{bmatrix} \\ &\quad + \begin{bmatrix} a_C & \omega \\ -\omega & a_C \end{bmatrix} \begin{bmatrix} i_D^* \\ i_Q^* \end{bmatrix} \\ &= \begin{bmatrix} -a_C & -\omega \\ \omega & -a_C \end{bmatrix} \begin{bmatrix} i_D \\ i_Q \end{bmatrix} + \begin{bmatrix} a_C & \omega \\ -\omega & a_C \end{bmatrix} \begin{bmatrix} i_D^* \\ i_Q^* \end{bmatrix}\end{aligned}\quad (5)$$

The closed loop poles for this system,  $s_{1,2} = -a_C \pm j\omega$ , are complex, denoting that there is cross coupling. The cross coupling in the proposed system can also be seen from the Bode plots shown in Figure 4 and Figure 5 for the closed loop transfer functions  $I_D(s)/I_D^*(s)$  and  $I_D(s)/I_Q^*(s)$  respectively.

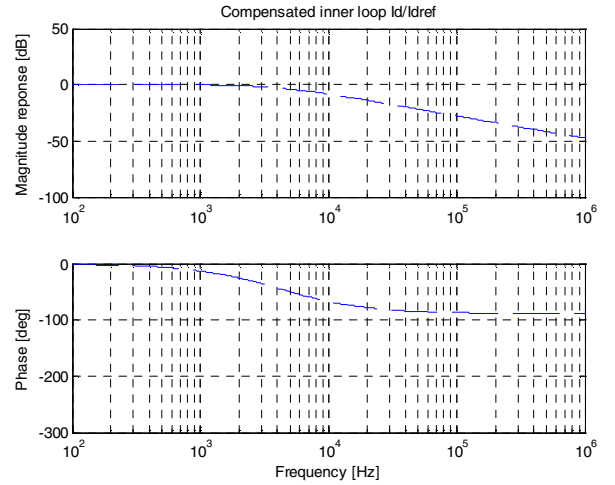


Figure 4 Bode plot of  $I_D(s)/I_D^*(s)$

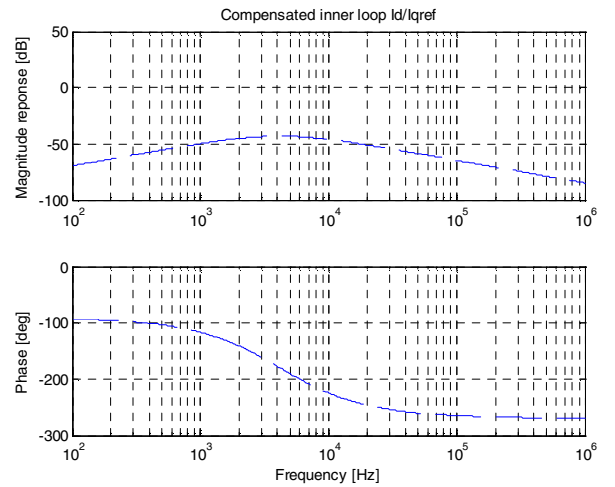


Figure 5 Bode plot of  $I_D(s)/I_Q^*(s)$

These are results with an inner loop bandwidth of  $f_{ci} = 4.2\text{kHz}$ . The transfer functions for  $I_Q(s)/I_Q^*(s)$  and  $I_D(s)/I_D^*(s)$  are identical. In a completely decoupled system, for example with full state feedback with no errors in the model, the latter transfer function would be zero.

The proposed method requires different feedback and pre-filter matrices  $G_i^a$  and  $K_i^a$  in the control signal  $\mathbf{p}$ , i.e.

$$\mathbf{p} = G_i^a k_e \mathbf{i} + K_i^a \mathbf{r} + R_i k_e \mathbf{e}$$

The resulting closed loop system equations are

$$\begin{aligned} \frac{d\mathbf{i}}{dt} &= A_i \mathbf{i} + B_i k_p \mathbf{p} + F_i \mathbf{e} \\ &= (A_i + B_i k_p G_i^a k_e) \mathbf{i} + B_i k_p K_i^a \mathbf{r} + (B_i k_p R_i k_e + F_i) \mathbf{e} \end{aligned}$$

Setting this equal to the desired system equations in (5), the matrices are determined as

$$G_i^a = \frac{a_c L}{k_p k_e} \mathbf{I} = k_g \mathbf{I}$$

and

$$K_i^a = \frac{L}{k_p} \begin{bmatrix} -a_c & -\omega \\ \omega & -a_c \end{bmatrix}$$

The diagonal terms are the same as for full state feedback, but the off-diagonal terms are now zero in  $G_i^a$  and non-zero in  $K_i^a$ . This removes the need for off-diagonal terms in the feedback, allowing it to be implemented in the  $abc$  frame, and requires off-diagonal terms in the pre-filter  $K_i^a$ , which is easily achieved since these terms are introduced by the slower outer loop in the synchronous  $dq$  frame.

$$\begin{aligned} \mathbf{p}_{abc} &= T_s^{-1} T_e^{-1}(\theta) k_g \mathbf{I} T_e(\theta) T_s k_c \mathbf{i}_{abc} \\ &\quad + T_s^{-1} T_e^{-1}(\theta) K_i^a \mathbf{r} + k_r k_e \mathbf{e}_{abc} \\ &= k_g k_c \mathbf{i}_{abc} + T_s^{-1} T_e^{-1}(\theta) K_i^a \mathbf{r} + k_r k_e \mathbf{e}_{abc} \end{aligned}$$

The implementation is much simpler than for full state feedback, as shown in Figure 6.

Figure 7 shows the measured loop gain and phase margin for the aforementioned active rectifier with a switching speed of 18 kHz. The crossover frequency  $f_{ci}$  is just above 5 kHz, therefore close to the design target of 4.2 kHz, and the phase margin is approximately  $60^\circ$ .

The proposed system is only approximately decoupled, and will perform at its worst during transient conditions when  $i_D$  and  $i_Q$  are not equal to the references  $i_D^*$  and  $i_Q^*$ . However, with a fast enough response time, the overall effect on outer loop system performance is expected to be minimal.

The calculated step response to a  $-100\text{A}$  step in  $i_Q^*$  for the system in equation 5 with the proposed approximation to full state feedback is shown in Figure 8. There is a perturbation in  $i_D$  with the approximation to full state feedback which would

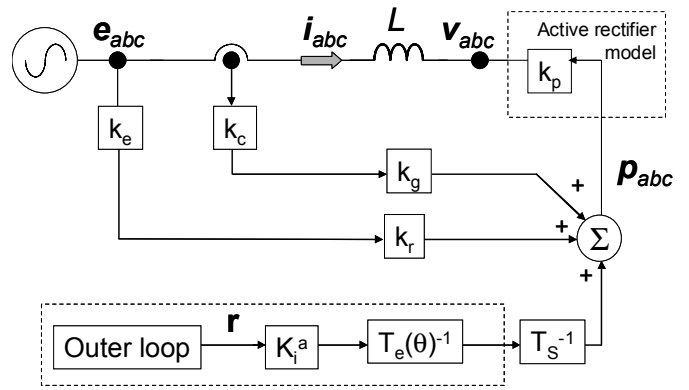


Figure 6 The proposed approximation to full state feedback

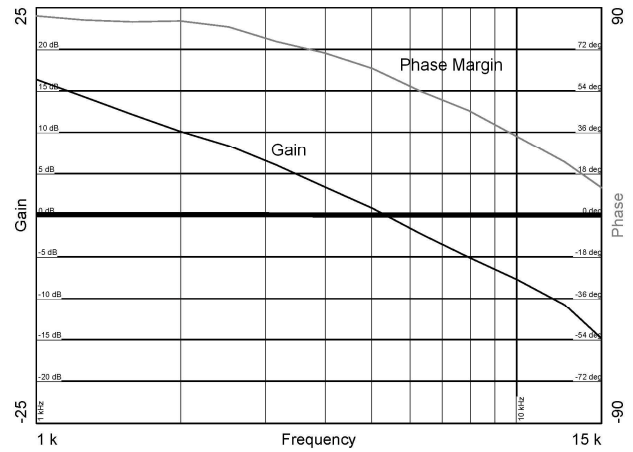


Figure 7 Measured inner loop gain and phase plot

not be present in a properly designed full state feedback system with an accurate system model. The perturbation is fairly small, with a peak value of approximately 1A.

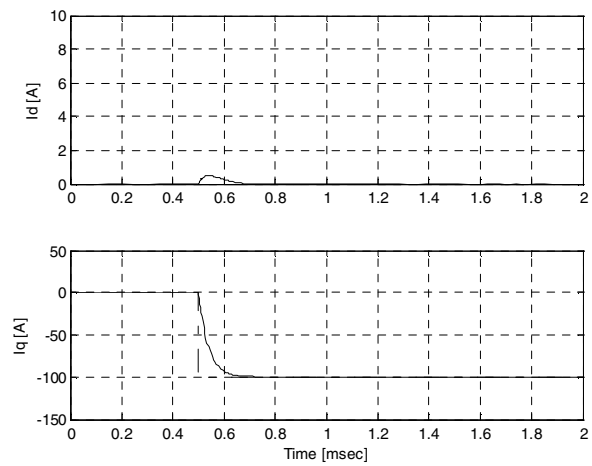


Figure 8 Calculated response to a  $-100\text{A}$  step in  $i_Q^*$

#### IV. EXPERIMENTAL RESULTS

A 300A, 480V active rectifier, shown in Figure 9, was developed where an inner loop control system was implemented as an approximation to full state feedback. Key specifications and design parameters are provided in Table I.

The measured response to a  $-100\text{A}$  step in  $i_Q^*$  is shown in Figure 10. The currents were measured in the  $abc$  frame and post processed to determine the  $dq$  components. It can be seen that the perturbation in  $i_D$  is considerably larger than calculated, peaking at approximately 10A.

TABLE I  
ACTIVE RECTIFIER DESIGN PARAMETERS

Maximum line current	300Arms
Maximum real power @ 480VAC	$\pm 250\text{kW}$
Maximum reactive power	$\pm 100\text{kVAR}$
Switching frequency	18 kHz
Line reactors	900 $\mu\text{H}$
DC Capacitor	2700 $\mu\text{F}$

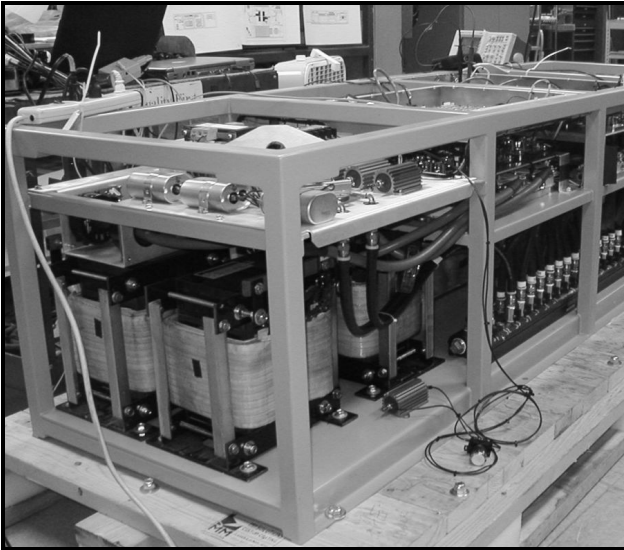


Figure 9 250 kW Active Rectifier

This discrepancy was found to be due to duty cycle saturation. It has been assumed thus far in modeling the system that it is linear, which is not the case. An important non-linearity in the system is saturation of the duty cycle in the PWM generation. The measured PWM signal saturation is shown in Figure 11 for the  $-100\text{A}$  step in  $i_Q^*$ .

This saturation effect can be modeled in the state space description by limiting the amplitude of the control signal  $\mathbf{p}$ , to the peak voltage of the sawtooth  $V_{saw}$ , i.e.

$$\text{if } |\mathbf{p}| = \sqrt{p_D^2 + p_Q^2} > V_{saw}$$

$$\text{then } \mathbf{p} = \frac{\mathbf{p}}{|\mathbf{p}|} \times V_{saw}$$

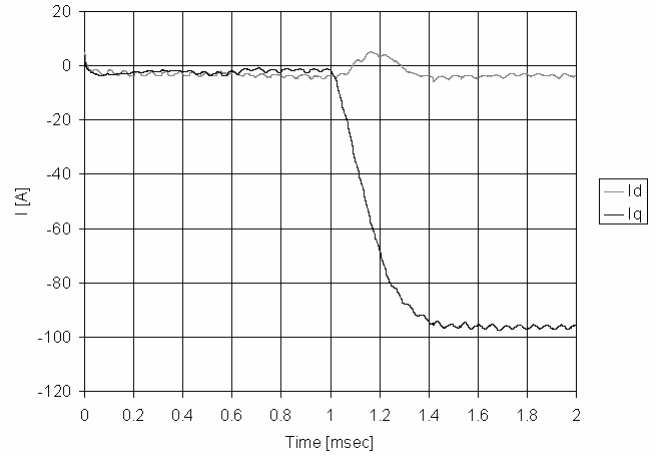


Figure 10 Measured response to a  $-100\text{A}$  step in  $i_Q^*$

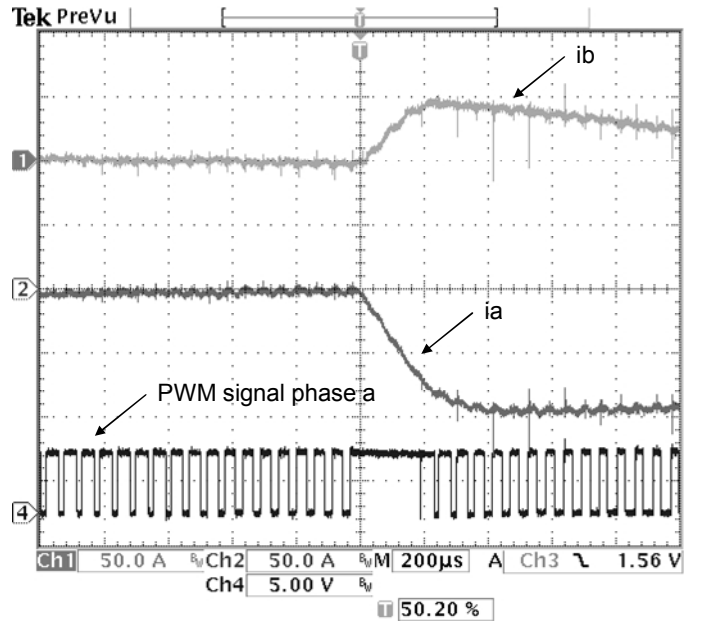


Figure 11 Measured PWM signal saturation

## V. PROCESSING BURDEN

The calculated step responses to a  $-100\text{A}$  step in  $i_Q^*$  for full state feedback, and the proposed approximation to full state feedback, both with a bandwidth of  $f_{ci} = 4.2\text{ kHz}$ , with and without duty cycle saturation modeled, are shown in Figure 12 and Figure 13 respectively. Note that a perfect model for the system is assumed here. While the full state feedback provides complete decoupling without saturation, the duty cycle saturation results in a significant excursion in  $i_D$ . While the proposed approximation to full state feedback does not result in a decoupled system, the excursion in  $i_D$  due to imperfect decoupling is significantly smaller than that caused by duty cycle saturation.

Since duty cycle saturation is a non-linear effect, it is more pronounced at larger reference input steps. Hence for small step changes, the performance of full state feedback would be better than the proposed approximation.

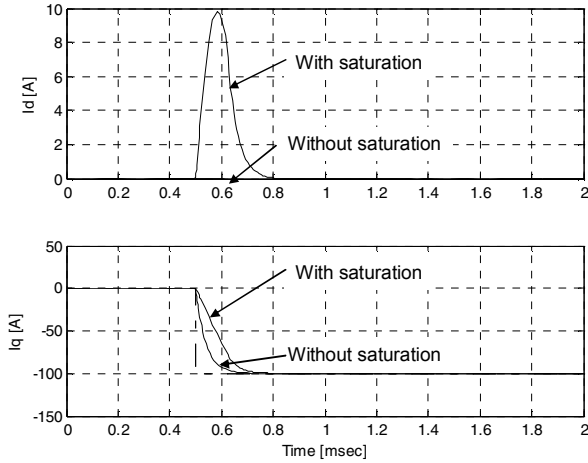


Figure 12 Calculated step response with full state feedback

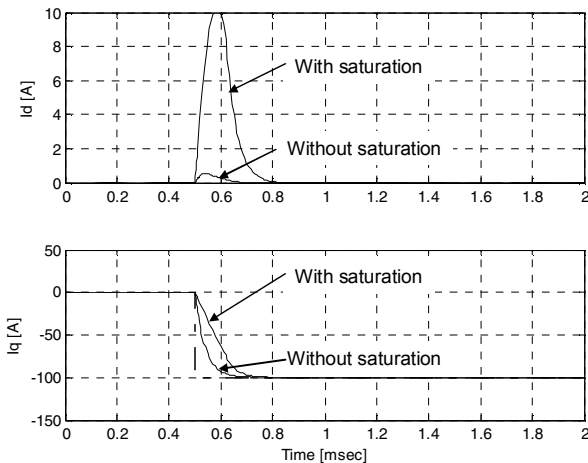


Figure 13 Calculated step response with proposed method

The proposed scheme does not impose a sampling frequency requirement on the system, since there is no sampling in the loop. The sampling rate is driven by outer loop requirements, with bandwidth  $f_{co} = 160\text{Hz}$ , which would drive a sampling rate of at least  $8 \times 160\text{Hz} = 1.28\text{ kHz}$ , which is significantly lower than the sampling rate driven by full state feedback in the inner loop of  $36\text{kHz}$  for comparable inner loop bandwidth.

Conversely in this experiment, given that the outer loops and therefore the reference currents  $\mathbf{r}$  for the inner loops, are updated every process interval ( $128\ \mu\text{sec}$  in this experiment, of which  $\sim 45\ \mu\text{sec}$  is used for primary loop processing), were the inner loop functions to be incorporated in the digital controller, inner loop speed would be largely a function of the loop apparatus (data acquisition and processor). While the addition of the inner loop functions into what is presently performed by the DSP would not greatly increase the number of required operations, running the inner loops with such a processing interval would slow inner loop bandwidth to

$$f_{ci} < \frac{1}{8} \times \frac{1}{128\ \mu\text{sec}} = \frac{7.8\text{kHz}}{8} = 976\text{ Hz}$$

This is almost a factor of five slower than that possible with the proposed method. As a consequence, significantly faster data acquisition and digital processing is required to implement a comparably fast full state feedback controller.

## VI. CONCLUSIONS

This paper has proposed a cost effective inner current loop control method for an active rectifier which is an approximation to full state feedback. Calculated and experimental results from a  $250\text{kW}$  prototype have been presented that show minimal differences in performance to full state feedback systems. Theoretical and experimental results indicate that steady state performance is identical, with transient response and saturation effects differing only slightly. Comparison of processing burden suggests that high speed data acquisition and processing requirements may be avoided or relaxed in favor of easily implemented Type 0 op-amp controllers.

## VII. REFERENCES

- [1] C. Schauder and H. Mehta, "Vector analysis and control of advanced static VAR compensators", IEE Proceedings-C, vol. 140, no. 4, pp. 299 – 306, July 1993.
- [2] R. Uhrin and F. Profumo, "State feedback current regulator for quasi direct AC/AC converter", EDPE 1996, Stara Lesna, Slovakia, pp. 79 – 84.
- [3] R. Uhrin and F. Profumo, "Complete state feedback control of quasi direct AC/AC converter", IEEE-IAS Annual Meeting, 1996, vol. 2, pp.1203 – 1209.
- [4] K. Ogata, *Modern Control Engineering*, 2<sup>nd</sup> Ed., Prentice-Hall, London, 1990.